ORIGINAL ARTICLE

CONTENTS

Possible somatosensory modulation of tinnitus in a patient with temporomandibular joint disorder: An fMRI/TMJ-MRI case report (3-Month Follow-Up)

Vasil Pehnyo[1], Nataliia Savychuk[1], Oleksandr Bida[2], Stanislav Riebienkov[3], Ivan Riabko[4], Roman Sulik[1]

[1]SHUPYK NATIONAL HEALTHCARE UNIVERSITY OF UKRAINE, KYIV, UKRAINE

[2]BOGOMOLETS NATIONAL MEDICAL UNIVERSITY, KYIV, UKRAINE

[3] NATIONAL CHILDREN'S SPECIALIZED HOSPITAL "OKHMATDYT", KYIV, UKRAINE

[4]TARAS SHEVCHENKO NATIONAL UNIVERSITY OF KYIV, KYIV, UKRAINE

ABSTRACT

Aim: To explore whether changes in mandibular/condylar position are associated with alterations in brain activation in a patient with chronic subjective tinnitus and temporomandibular disorder (TMD) during a 3-month follow-up.

Materials and Methods: Single-patient case report (39-year-old; 2-year tinnitus; diagnosed TMD). TMJ magnetic resonance imaging (TMJ MRI) and functional magnetic resonance imaging(fMRI) of the brain were acquired in centric occlusion and after fabrication of an anterior repositioning appliance. fMRI was processed in FMRIB Software Library (FSL) (FEAT 6.0); Z-images were cluster-corrected with $Z>3.1$ and cluster-wise $p<0.05$ (Gaussian random field theory). Primary metrics: Activation Index (AI; Z-max), cluster size (voxels). Discriminative ability between states was explored with ROC analysis.

Results: Mean (AI) decreased from 5.51 ± 0.67 (occlusion) to 5.05 ± 0.70 (splint), $p<0.05$. A large cluster in the left superior temporal gyrus present in occlusion (AI=6.54; 16 799 voxels) disappeared with the splint. Regional reductions were also observed in anterior cingulate and prefrontal/insular cortices, while some right temporal/frontal clusters persisted with lower AI. Receiver Operating Characteristic (ROC) analysis suggested the AI (Z-max) had the highest discriminative ability between states (Area Under the Curve (AUC)$\approx$0.69), whereas voxel-wise uncorrected/false discovery rate(FDR)-corrected p values were weak classifiers.

Conclusions: In this clinical case, mandibular repositioning with an anterior repositioning appliance was associated with decreased cortical hyperactivation in auditory/affective regions and disappearance of a major left temporal cluster. Findings support a plausible somatosensory contribution to tinnitus modulation in TMJ disorder and motivate hypothesis-driven prospective studies. Causality cannot be inferred from a single-case design.

KEY WORDS: tinnitus, temporomandibular joint disorders, fMRI, TMJ MRI, anterior repositioning appliance, somatosensory tinnitus

Wiad Lek. 2026;79(2):300-309. doi: 10.36740/WLek/214420 DOI

INTRODUCTION

Subjective tinnitus is a disorder often associated with increased neural activity in the central auditory system and related areas of the brain [1-8]. In recent decades, functional MRI (fMRI) studies have made it possible to better understand the neurophysiological basis of tinnitus, in particular the mechanisms underlying its reduction or intensification in patients [9], and a strong association between TMD and tinnitus; one meta-analysis reported ~4.45-fold higher odds of tinnitus in individuals with TMD than in those without [10]

In the general population, the prevalence of tinnitus ranges from 15-20% to 44.5%.In patients with Temporomandibular Disorders (TMD), this figure can increase from 25 to 59%, which indicates a possible association between these conditions [10, 11, 14]. Such a high level of prevalence emphasizes the need for a deeper study of both the pathophysiological mechanisms of tinnitus and the associated risk factors, including TMD. At the present stage, numerous studies confirm that the TMD can significantly influence the occurrence and course of tinnitus through somatosensory and neuronal integration [10-12, 15, 16].

Despite the number of scientific studies, the role of the TMD in the development of tinnitus has not yet been sufficiently studied. Consideration of such clinical cases allows not only to better understand the pathophysiology of tinnitus, but also emphasizes the importance of a multidisciplinary approach to the diagnosis and treatment of this disorder. This is especially true in the context of the latest findings, which demonstrate the complex interaction of somatic and neuronal mechanisms in the formation of symptoms [8, 10, 16, 17].

Scientists distinguish the following mechanisms of tinnitus development in patients with TMD: somatosensory, reflex, muscular, anatomical, psychophysiological, central sensitization. Particular attention is paid to the role of central sensitization, which, according to recent studies, can increase the activity of the auditory tracts even in the absence of external stimuli [13, 14, 17]. For example, studies using fMRI have found increased activity in the auditory and sensorimotor areas of the cerebral cortex in patients with tinnitus, suggesting a complex neuronal mechanism of this disorder [15, 18-23].

In our opinion, among the theories presented, the competence of a dentist may include somatosensory, reflex, anatomical, muscular hypotheses.

AIM

To explore whether changes in mandibular/condylar position are associated with alterations in brain activation in a patient with chronic subjective tinnitus and temporomandibular disorder (TMD) during a 3-month follow-up.

MATERIALS AND METHODS

Patient O., born in 1985, applied to the Department of Orthopedic Dentistry, Digital Technologies and Implantology, Faculty of Dentistry of the Shupyk National Health University of Ukraine on October 22, 2024 with complaints of a constant feeling of tension in the jaw and bruxism, as well as a subjective feeling of constant tinnitus, which has been observed over the past 2 years, after collecting complaints and anamnesis.

After filling out the normative consent and familiarizing himself with the examination plan (approved *by the Commission on Ethics and Academic Integrity of the* Shupyk National Health University of Ukraine (protocol No. 13/10), an examination was carried out according to the generally accepted methodology. The treatment tactics were as follows, taking into account the neurological component, the use of an interdisciplinary approach involved specialists in related specialties, including a neurologist and an orthopedist. This strategy allows us to take into account the relationship between somatosensory symptoms and neurophysiological mechanisms of tinnitus [20-22].

A anterior repositioning appliance on the upper jaw was fabricated to achieve the therapeutic reference position(TRP) according to Gelb/Lotzmann principles. TRP was determined by symptom-guided deprogramming with Kois deprogrammer[28], bilateral palpation, and verification of reduced joint loading and muscle tenderness. The appliance was made from hard acrylic dental material; with uniform lingual occlusal contacts and anterior guidance preventing posterior interferences. The patient was instructed to wear the device nighttime only for at least 12 weeks, with check-ups at 1,3,10 and 12 weeks for occlusal equilibration. Adherence and adverse events were recorded.

Additional diagnostic of the state of the TMJ were carried out using MRI of the TMJ and determination of the activity of the cerebral cortex using fMRI of the brain, after the manufacture of a repositioning appliance on the upper jaw.

The results of the audiogram (Fig. 1) indicate normal hearing in the patient. The right ear has hearing thresholds for air conduction (AC) in the range of up to 20 dB at all frequencies, and bone conduction (BC) is also in the range of up to 20 dB, indicating normal air and bone conduction. Similarly, the left ear shows hearing thresholds for AC and BC up to 20 dB at all frequencies. on palpation at the level of C6-C7, percussion of the spinous processes, sharp pain, palpation of paravertebral T5-T6 on the left sharply painful, painful rotation. Clinical diagnosis: facet syndrome T5-T6 on the left, C6-C7 on the left. Tinnitus.

The examination according to the generally accepted method revealed the presence of integral dentition, the CPV index was 23%, the bite was orthognathic, hypermobility of the articular heads on both sides was noted, without signs of scaling and (or) crepitus.

Functional diagnosis of TMJ included magnetic resonance imaging (MRI), which was performed in the position of centric occlusion and open mouth, for a detailed analysis of the biomechanics of the joint[16]. The MRI of the TMJ and fMRI of the cerebral cortex was performed on a Siemens MAGNETOM Aera (1.5 Tesla) device with a 12-channel head coil.

The results of MRI of the TMJ in the position of centric occlusion were found in the right TMJ: Degeneration and partial rupture of the intermediate part of the articular disc, compression of the articular disc. Minimal anterior displacement of the disc, violation of the biomechanics of the joint. Left TMJ: Degeneration and erosion of the intermediate part of the articular disc, compression of the articular disc. Minimum anterior displacement (Fig. 2).

After analyzing the complaints and laboratory research methods carried out, it was decided to determine the curative position for TMJ, according to the theory of Gelb (1960)[18]. Next, a anterior repositioning appliance was made for the upper jaw. The treatment tactics corresponded to modern approaches to the treatment of TMJ dysfunction, based on the stabilization of occlusion and the restoration of joint function.

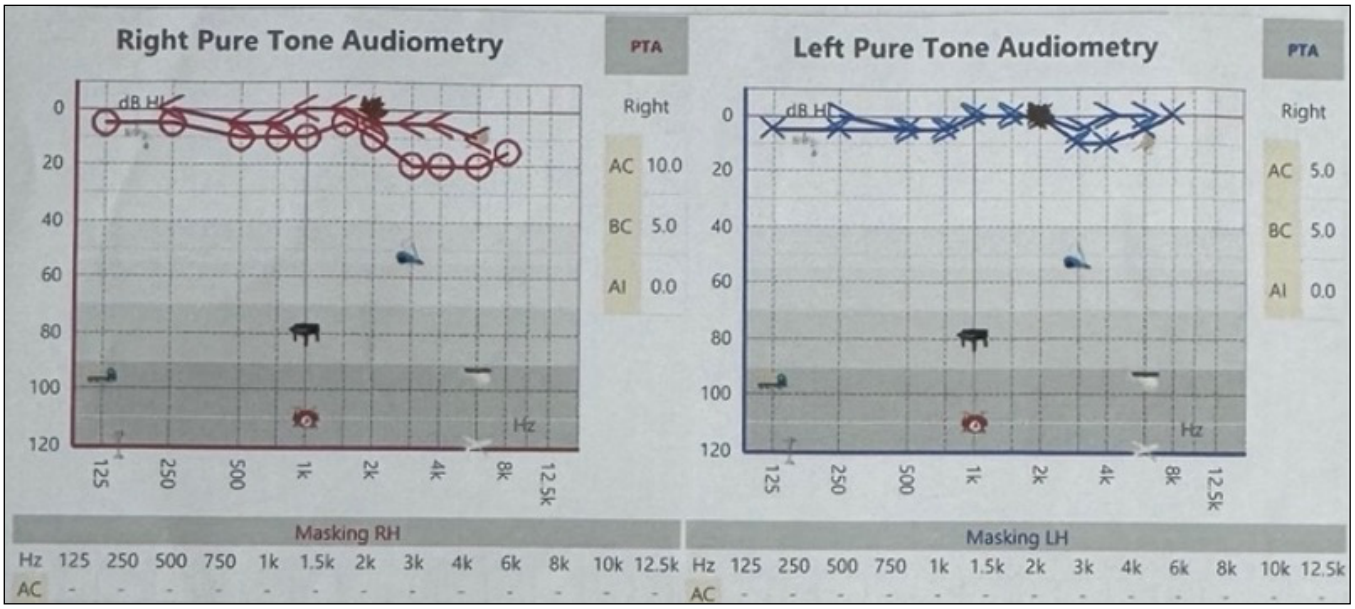

Fig. 1. Results of the audiogram of the examined patient
Picture taken by the authors

In particular, the theories of Gelb (1960) and Lotzmann (1980-1990) were used, which predict reducing the load on the affected joint by optimizing the position of the lower jaw [19].

The results of MRI of the TMJ in the position with the repositioning splint were found in the right TMJ: degeneration and partial rupture of the intermediate part of the articular disc, lack of compression of the articular disc. Reduction of anterior displacement of the disc. Left TMJ: Degeneration and erosion of the intermediate part of the articular disc, lack of compression of the articular disc. Reduction of the minimum anterior displacement (Fig. 3).

RESULTS

Analysis of statistical indicators for the "Occlusion" and "Splint" states revealed the following features: in "Occlusion", the mean Activation index (AI) z-max is 5.51(mean=5.51) with a standard deviation of 0.67(σ=0.67), and the Number of voxels in cluster has an average of 3086 (mean=3086) with a large standard deviation of 3842(σ=3842), which indicates a lot of variability. For the "Splint" position, the mean activation index is lower at 5.05(mean=5.05) with a standard deviation of 0.70(σ=0.70), with the number of voxels in the cluster also varying significantly, with a mean of 3166(mean=3166) and a standard deviation of 7859(σ=7859). These data indicate within-subject differences between the two jaw-position states in this patient's brain activity. The results of the fMRI examination are presented in Table 1 and Table 2.

Following the obtained fMRI statistics, fMRI data processing was carried out using the FEAT (FMRI Expert Analysis Tool) software package version 6.00, which is part of the FSL (FMRIB's Software Library) Statistical images Z (T/F Gaussianized) were threshold using clusters defined by Z>3.1 and the (adjusted) cluster significance threshold P=0.05[26]. This was followed by a statistical analysis for logistic regression (the position of the lower jaw was determined by an independent change, the fMRI indicators were used as a metric both for the usual closure of the teeth and for the position after treatment), and an ROC curve was constructed for the sample of diagnostic-effective indicators of the fMRI study (Fig. 4).

The resulting ROC curves indicated the diagnostic efficacy of five fMRI scores for classification between Splint (control) and Occlusion (pathology) conditions, where each significant cluster was considered as a separate observation. The highest discriminatory ability was shown by the Activation index (AI) Z-MAX) with an AUC ≈ 0.69, which indicates its high information content. Number of voxels in cluster (AUC ≈ 0.60) and Corrected p value, whole cluster -ln(P) (AUC ≈ 0.64) had lower but moderate classification ability. False Discovery Rate-corrected p value of voxel (AUC ≈ 0.37) and Uncorrected p value of voxel (AUC ≈ 0.36) turned out to be statistically weak and practically do not allow to distinguish between groups.

Thus, among the proposed results of fMRI, Activation index, Corrected p value whole cluster -ln(P) and Number of voxels in cluster can be considered as key markers[26, 27].

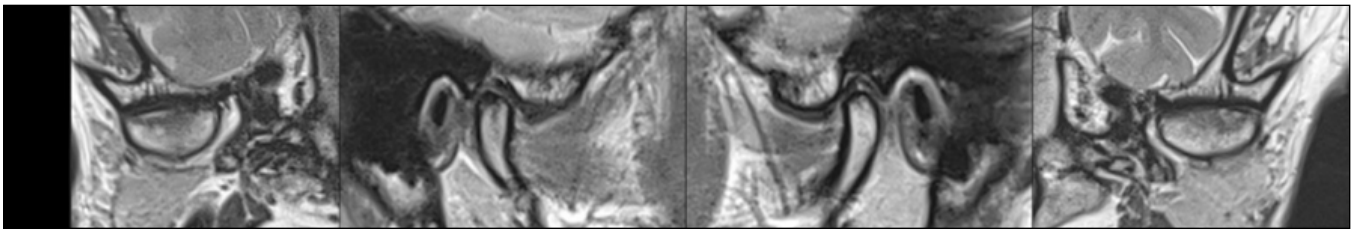

Fig. 2. MRI-TMJ _right and left in the paracoronary and parasagittal planes
Picture taken by the authors

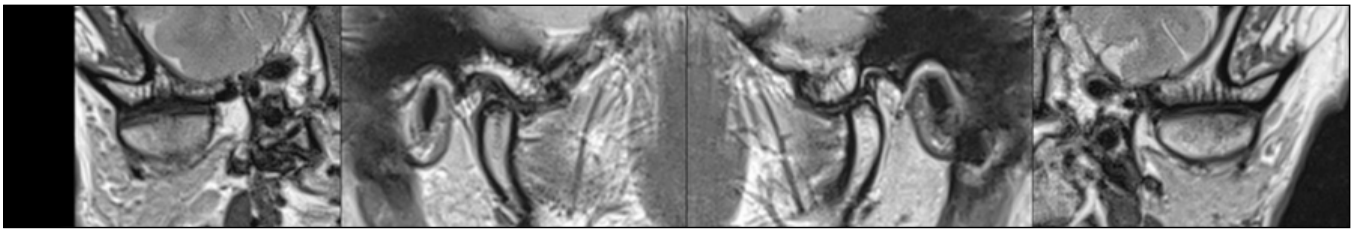

Fig. 3. MRI-TMJ _right and left in the paracoronary and parasagittal planes
Picture taken by the authors

It should be noted that the data obtained were obtained with the cluster-forming threshold Z>3.1; observed Z-max up to 7.5; cluster-wise FWE p<0.05 (GRF).

The assessment of changes in functional activation between the Occlusion and Splint states by *the Activation index (AI) Z-MAX* and *Number of voxels in cluster revealed* significant topographic and quantitative differences in the following anatomical areas:

1. **The Right Superior Temporal Gyrus** is activated in both states with a higher AI Z-max in Occlusion at 1.08 (6.76 vs 5.68), with a slight decrease in the number of voxels by 289 (5344 vs 5633).
2. **The Right Superior Frontal Gyrus** shows an increase in AI Z-max of 1.92 (6.41 vs 4.49) and an increase in the number of voxels by 4433 (5334 vs 901) in the Occlusion state
3. **Left Superior Temporal Gyrus** is only activated in Occlusion with AI Z-max 6.54 and a voxel count of 16799, completely absent in Splint
4. **The Left Anterior Cingulate Cortex** is only seen in Occlusion with AI Z-max 5.62 and 10269 voxels, while Splint lacks this activation.
5. **Right Temporal Pole** only appears in Splint with AI Z-max 4.87 and 1594 voxels, missing from Occlusion
6. **Left Middle Temporal Gyrus** is only activated in Splint with AI Z-max 5.16 and 1315 voxels, not detected in Occlusion
7. **Right Precentral Gyrus** is only present in Splint with AI Z- max 5.11 and 1203 voxels
8. **Left Insula** is observed in Splint with AI Z-max 4.63 and 1132 voxels, inactive in Occlusion
9. **Right Middle Frontal Gyrus** is only active in Splint, has AI Z-max 5.08 and 1062 voxels
10. **Right Paracentral Lobule** only appears in Splint with AI Z-max 4.79 and 843 voxels
11. **Left Superior Frontal Gyrus** is only activated in Splint with AI Z-max 4.52 and 728 voxels.

DISCUSSION

In this single-patient fMRI/TMJ-MRI case with a within-subject comparison of Occlusion versus Splint states, mandibular repositioning was associated with a measurable reduction in cortical activation metrics, including a decrease of the mean Activation Index (AI; Z-max) and the disappearance of a very large Left Superior Temporal Gyrus cluster that was present in occlusion.

These findings are consistent with the broader neuroimaging literature suggesting that tinnitus is not limited to a single "auditory locus" but involves distributed changes across auditory and non-auditory networks, including cortical regions implicated in auditory perception, attention, salience, and affective processing [3–7,20,21]. Contemporary frameworks derived from human neuroimaging emphasize network-level contributions to tinnitus perception and persistence, including maladaptive patterns of local activity and altered connectivity across cortical systems [3,6,20,21]. Our observation that the Left Superior Temporal Gyrus cluster (auditory association territory) was prominent in occlusion and then absent in the splint state aligns with reports that tinnitus can be accompanied by abnormal cortical activity patterns in auditory areas and that these patterns may vary with state-dependent modulation [2–4,7,20,21]. Although causality cannot be inferred, the directionality of change (reduced activity markers

Table 1. Results of fMRI of the brain before treatment (highlighted in color according to ROC analysis)

Anatomical region	Activation index (AI) Z-MAX	Corrected p value. whole cluster -ln(P)	Number of voxels in cluster	False Discovery rate-corrected p-value of voxel	Uncorrected p-value voxel	Talairach Daemon Atlas Coordinates mni		
						x	y	z
Left Cerebrum. Temporal Lobe. Superior Temporal Gyrus. White Matter.	6.54	23.4	16799	0.000	4.15e-24	-60	-48	155
Left Cerebrum. Limbic Lobe. Anterior Cingulate. White Matter.	5.62	16.4	10269	0.000	4.06e-17	-13	35	19
Right Cerebrum. Temporal Lobe. Superior Temporal Gyrus. White Matter.	6.76	10	5344	0.000	9.16e-11	66	-20	4
Right Cerebrum. Frontal Lobe. Superior Frontal Gyrus. White Matter.	6.41	10	5334	0.000	9.47e-11	67	179	91
Left Cerebrum. Temporal Lobe. Fusiform Gyrus. White Matter.	6.35	9.43	4929	0.000	3.74e-10	-53	-8	-31
Right Cerebrum. Temporal Lobe. Inferior Temporal Gyrus. White Matter.	5.54	7.65	3789	0.000	2.23e-08	54	-9	-33
Left Cerebrum. Occipital Lobe Middle. Temporal Gyrus. White Matter.	5.34	7.59	3750	0.000	2.58e-08	-52	-73	19
Right Cerebrum. Frontal Lobe. Medial Frontal Gyrus. White Matter.	5.14	3.8	1689	0.000	0.00016	14	59	-2
Left Cerebrum. Occipital Lobe. Cuneus. Gray Matter. Brodmann area 18.	5.68	3.67	1631	0.001	0.000213	-11	-70	17
Left Brainstem. Midbrain.	5.61	3.39	1501	0.001	0.00041	-11	-20	9
Left Cerebrum. Parietal Lobe. Sub-Gyral. White Matter.	5.92	3.29	1456	0.001	0.000516	-25	-34	59
Right Cerebrum. Frontal Lobe. Sub-Gyral. White Matter.	5.65	3.06	1355	0.002	0.000874	20	11	55
Right Cerebrum. Temporal Lobe. Superior Temporal Gyrus. Gray Matter. Brodmann area 39.	4.35	3.01	1336	0.002	0.000967	57	-61	23
Left Cerebrum. Limbic Lobe. Uncus. White Matter.	5.9	2.78	1237	0.003	0.00165	-31	-1	-25
Left Cerebrum. Frontal Lobe. Medial Frontal Gyrus. Gray Matter. Brodmann area 6.	5.98	2.61	1166	0.004	0.00243	-3	1	57
Left Cerebrum. Frontal Lobe. Sub-Gyral. White Matter.	5.12	2.5	1120	0.004	0.00314	-31	-13	43
Left Cerebrum. Frontal Lobe. Superior Frontal Gyrus. Gray Matter. Brodmann area 6.	5.23	2.49	1114	0.004	0.00325	-16	22	55
Right Cerebrum. Limbic Lobe. Posterior Cingulate. Gray Matter. Brodmann area 30.	4.43	1.91	886	0.015	0.0123	5	-47	16
Right Cerebellum. Posterior Lobe. Pyramis. Gray Matter.	4.94	1.8	845	0.018	0.0158	48	-83	55
Left Brainstem. Pons.	4.6	1.78	835	0.018	0.0168	-10	-31	-34
Left Cerebrum. Parietal Lobe. Precuneus.	5.1	1.7	808	0.021	0.0198	90	56	115
Left Cerebellum. Posterior Lobe. Declive. Gray Matter.	4.91	1.42	707	0.038	0.0376	115	57	52

Note:

Activation index (AI) Z-MAX - a numerical variable that displays the maximum activation index value in a given region of the brain.

Number of voxels in cluster - the number of voxels in the cluster where statistically significant activation is observed. A higher number of voxels may indicate a more significant change in brain activity.

Corrected p value, whole cluster -ln(P) is the logarithm of the negative value of the corrected p-value for the whole cluster. A lower value of p indicates a greater statistical significance of changes in brain activity.

False Discovery rate-corrected p value of voxel - thecorrect value of p for the voxel, adjusted according to the False Discovery Rate (FDR) control method, which reduces the likelihood of false positives.

Uncor-rected P value voxel - p-value calculated for a specific voxel without correction for multiple comparisons.

Talairach Daemon Atlas Coordinates mni – coordinates, according to the parameters of mni and the Tailarach atlas

Source: compiled by the authors of this study

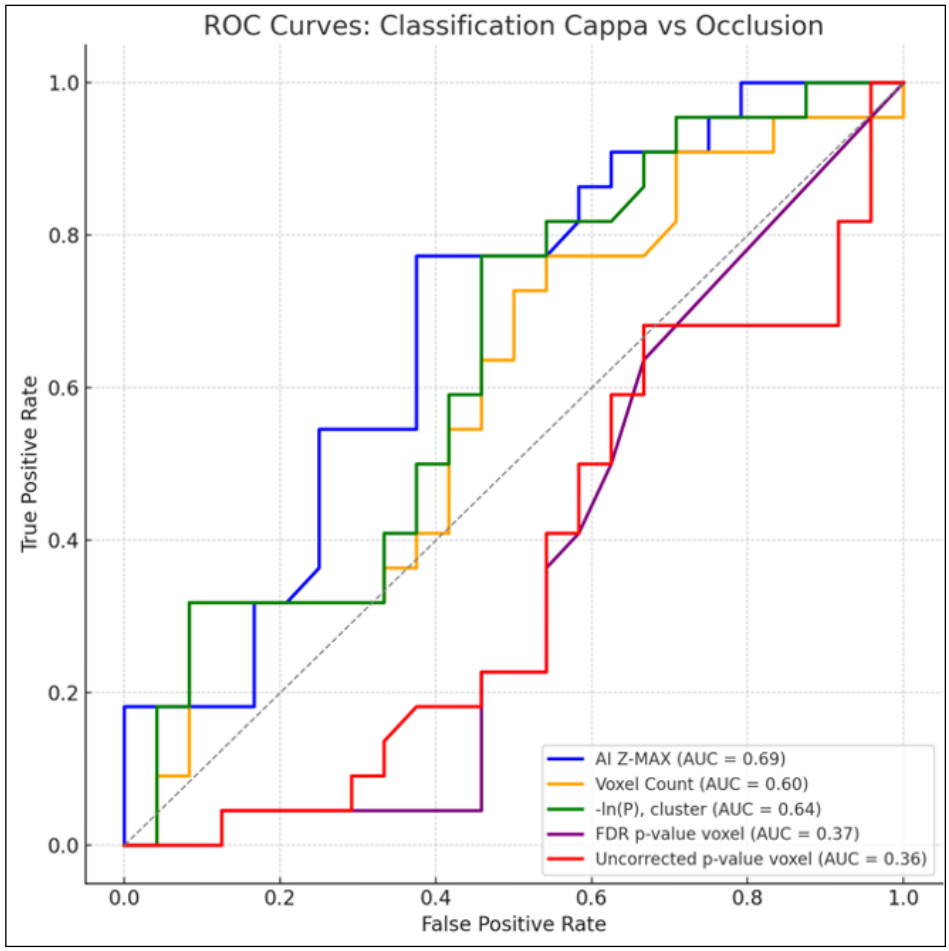

Fig. 4. ROC-Curves fMRI results
Picture taken by the authors

with mandibular repositioning) is compatible with the concept that at least some tinnitus phenotypes may express a modifiable cortical signature under specific physiological or somatosensory conditions [3,6,20,21].

Beyond auditory cortex, the affective and salience-related components of tinnitus are increasingly recognized as key determinants of distress and symptom burden [3,6,22,24]. In our case, Left Anterior Cingulate Cortex activation was present in occlusion and absent in the splint state, and regional reductions were also described in prefrontal/insular territories.

These findings are broadly concordant with the literature linking tinnitus-related distress and chronicity to engagement of limbic–cortical circuits and "aversive memory" or salience networks rather than purely peripheral auditory damage [22,24]. The ACC and frontal systems are often discussed as part of a distributed network supporting attention to internally generated percepts and the affective appraisal of tinnitus [3,20–22,24]. Therefore, attenuation of activity markers in these regions after mandibular repositioning may reflect a shift in the balance between auditory representation and top-down modulatory control, a pattern that is conceptually compatible with network models proposed in neuroimaging reviews and meta-analyses [3,20,21].

The clinical context—temporomandibular disorder with tinnitus—also supports interpreting the observed state-dependence through a somatosensory lens. Systematic reviews and meta-analyses consistently report an association between TMD and tinnitus and emphasize the clinical relevance of multidisciplinary evaluation for patients with orofacial complaints and ear symptoms [10–12,14,18]. In particular, contemporary evidence syntheses describe higher tinnitus prevalence/odds in individuals with TMD and underscore that somatosensory factors can influence tinnitus severity and treatment response [10–12,14,18]. Interventional literature similarly supports the plausibility of somatosensory tinnitus modulation: an RCT evaluating orofacial treatment within a multidisciplinary program and subsequent mechanistic work suggest that improving TMD status can mediate reductions in somatic tinnitus severity [8,9]. A broader systematic review of physical therapy interventions in subjective tinnitus further supports that targeting somatic contributors may be beneficial in selected patients [16], and recent controlled trials of manual therapy report effects on somatosensory tinnitus/dizziness outcomes [15]. Against this background, our within-subject fMRI

Table 2. Results of fMRI of the brain after treatment (highlighted in color according to ROC analysis)

Anatomical region	Activation index (AI) Z-MAX	Correced p-value, whole cluster -ln(P)	Number of voxels in cluster	False Discovery rate-corected p-value of voxel	Uncorreced p-value voxel	Talairach Daemon Atlas Coordinates mni		
						x	y	z
Left Cerebrum. Temporal Lobe. Superior Temporal Gyrus. Gray Matter Brodmann area 42.	5.86	40.5	39682	0.000	3.09e-41	-64	-26	17
Right Cerebrum. Temporal Lobe. Superior Temporal Gyrus. White Matter.	5.68	9.88	5633	0.000	1.33e-10	65	-36	11
Right Cerebrum. Frontal Lobe. Medial Frontal Gyrus. Gray Matter Brodmann area 6.	6.23	6.22	3171	0.000	5.96e-07	84	128	132
Right Cerebrum. Frontal Lobe. Superior Frontal Gyrus. Gray Matter Brodmann area 10.	4.81	6.02	3037	0.000	9.54e-07	28	58	18
Left Cerebrum. Frontal Lobe. Sub-Gyral. White Matter.	5.05	4.93	2411	0.000	1.18e-05	-28	40	-3
Left Cerebrum. Sub-lobar. Extra-Nuclear. White Matter.	5.48	4.55	2204	0.000	2.82e-05	-17	3	22
Left Cerebrum. Limbic Lobe. Parahippocampal Gyrus. White Matter.	4.98	4.22	2029	0.000	6.01e-05	-34	-21	-24
Left Cerebrum. Sub-lobar. Extra-Nuclear. White Matter. Corpus Callosum.	5.39	4.01	1921	0.000	9.7e-05	-14	31	6
Right Cerebrum. Parietal Lobe. Precuneus.	6	3.47	1650	0.001	0.000336	48	-76	43
Right Cerebrum. Frontal Lobe. Middle Frontal Gyrus. Gray Matter Brodmann area 6.	6.16	3.17	1502	0.002	0.00068	54	5	38
Right Cerebrum. Frontal Lobe. Middle Frontal Gyrus. Gray Matter Brodmann area 10.	3.93	2.82	1340	0.003	0.00151	46	46	13
Left Cerebrum. Occipital Lobe. Middle Occipital Gyrus. White Matter.	4.36	2.48	1189	0.007	0.00328	-44	-73	7
Right Cerebrum. Temporal Lobe. Inferior Temporal Gyrus. White Matter.	6.13	2.32	1119	0.009	0.00475	62	-53	-15
Inter-Hemispheric.	4.2	1.87	929	0.023	0.0135	1	-20	13
Right Cerebellum. Anterior Lobe. Gray Matter. Dentate	4.21	1.85	920	0.023	0.0142	16	-57	-23
Right Cerebrum. Frontal Lobe. Superior Frontal Gyrus. White Matter.	4.49	1.8	901	0.024	0.0158	24	52	-8
Right Cerebrum. Frontal Lobe. Precentral Gyrus White Matter.	5.45	1.76	886	0.024	0.0172	43	-6	55
Right Cerebrum. Parietal Lobe. Sub-Gyral. White Matter	4.98	1.6	822	0.032	0.025	32	-56	42
Left Cerebrum Temporal Lobe. Middle Temporal Gyrus. Gray Matter Brodmann area 39.	5.06	1.58	813	0.032	0.0263	-35	-62	31
Left Cerebrum. Frontal Lobe. Middle Frontal Gyrus.	4.31	1.57	810	0.032	0.0268	-43	45	17
Right Cerebrum. Sub-lobar. Claustrum. Gray Matter.	4.57	1.56	804	0.032	0.0277	32	17	5
Left Cerebrum. Temporal Lobe. Middle Temporal Gyrus. White Matter.	4.94	1.4	742	0.043	0.0401	-56	-56	2
Right Cerebrum. Frontal Lobe. Precentral Gyrus White Matter.	4.34	1.39	738	0.043	0.0411	33	-15	54
Right Cerebrum. Limbic Lobe. Cingulate Gyrus White Matter.	4.48	1.36	728	0.044	0.0436	11	16	24

Note:

Activation index (AI) Z-MAX - a numerical variable that displays the maximum activation index value in a given region of the brain.

Number of voxels in cluster - the number of voxels in the cluster where statistically significant activation is observed. A higher number of voxels may indicate a more significant change in brain activity.

Corrected p value, whole cluster -ln(P) is the logarithm of the negative value of the corrected p-value for the whole cluster. A lower value of p indicates a greater statistical significance of changes in brain activity.

False Discovery rate-corrected p value of voxel - thecorrect value of p for the voxel, adjusted according to the False Discovery Rate (FDR) control method, which reduces the likelihood of false positives.

Uncor-rected P value voxel - p-value calculated for a specific voxel without correction for multiple comparisons.

Talairach Daemon Atlas Coordinates mni – coordinates, according to the parameters of mni and the Tailarach atlas.

Source: compiled by the authors of this study

differences between jaw-position states provide a neuroimaging correlate that is directionally compatible with the clinical concept of somatosensory tinnitus in the setting of TMD [8–12,15,16,18].

At the same time, our results also highlight the complexity of brain responses to mandibular repositioning. Several regions were reported as present only in the splint state (e.g., Right Temporal Pole, Left Middle Temporal Gyrus, Right Precentral Gyrus, Left Insula, Right Middle Frontal Gyrus, Right Paracentral Lobule, Left Superior Frontal Gyrus), while some right temporal/frontal clusters persisted across both states with reduced AI.

Such patterns do not necessarily contradict "reduction of hyperactivity"; rather, they may indicate network reconfiguration in which decreases in dominant auditory/affective clusters co-occur with recruitment of regions involved in sensorimotor integration, attentional control, or contextual processing, which are frequently implicated in contemporary tinnitus network accounts [3,5,6,20,21,24]. Importantly, the neuroimaging literature emphasizes heterogeneity across tinnitus phenotypes and the need to interpret regional activations within broader network dynamics rather than as isolated markers [3,6,20,21]. Therefore, state-dependent emergence of additional clusters in the splint condition may represent compensatory or adaptive redistribution of processing demands, especially in a single-case design.

Methodologically, the use of cluster-based inference (cluster-forming threshold $Z>3.1$; cluster-wise significance control) is aligned with standard approaches to fMRI statistical mapping [25].

The exploratory ROC analysis indicated that AI (Z-max) showed the highest discriminative ability between states (AUC≈0.69), whereas voxel-wise p-value metrics were weak classifiers.

While AUC≈0.69 is only moderate by conventional diagnostic-accuracy interpretation [26], it is noteworthy in a within-subject, cluster-as-observation exploratory setting and supports prioritizing AI-like summary metrics in future hypothesis-driven work, as also discussed in methodological literature on ROC interpretation and performance quantification [26,27]. Overall, these analytic results support the notion that a small set of fMRI-derived summary indicators (AI, cluster-level measures) may be more stable for state discrimination than voxel-wise p-value features in this context [25–27].

This report has clear limitations. Most importantly, a single-case design precludes causal inference and generalization; spontaneous fluctuations, regression to the mean, and non-specific effects (including placebo-related mechanisms) may contribute to observed clinical or neural changes [17].

Additionally, tinnitus is heterogeneous, and neuroimaging findings vary across studies depending on inclusion criteria, hearing status, analytic pipelines, and the specific symptom dimension studied (perception vs distress vs comorbidities) [3,6,20,21]. For these reasons, the present observations should be viewed as hypothesis-generating. Future work should test preregistered hypotheses in prospective cohorts enriched for TMD-related/somatosensory tinnitus, incorporate standardized tinnitus outcomes alongside repeated neuroimaging time points, and examine whether changes in TMJ biomechanics on MRI covary with reproducible changes in network-level brain metrics [8–12,15,16,20,21]. Such studies would help clarify whether mandibular repositioning reliably modulates auditory–affective circuitry in a subset of patients and whether fMRI-derived markers such as AI can support monitoring of treatment-related neurofunctional change.

CONCLUSIONS

The mandibular position with the anterior repositioning appliance was associated with a decrease in the mean Activation Index (AI) in the brain - from 5.51 ± 0.67 to 5.05 ± 0.70 ($\Delta = -8.3\%$; $p<0.05$) - and the disappearance of a large cluster of the left superior temporal gyrus (16799 voxels), indicating a significant decrease in pathological neuronal hyperactivity associated with tinnitus. The exploratory discriminative signal of AI as a neuroimaging biomarker is confirmed by an AUC ≈ 0.69 (the highest among the five indicators), which makes it promising for monitoring the therapeutic effect in future studies. The most pronounced regional changes are observed in key auditory-sensory and affective areas, such as Right Superior Temporal Gyrus: $\Delta AI = 1.08$ with a slight decrease in cluster volume of 289 voxels, which may indicate a mitigation of pathological activation of the auditory pathways; Left Superior Temporal Gyrus: complete disappearance of ΔAI activation =6.54, which correlates with a probable decrease in subjective noise perception; Prefrontal Cortex: $\Delta AI = 1.92$ and contraction of the voxel cluster ($\Delta = 4433$), possibly increasing top-down inhibition and decreased emotional reactivity to tinnitus; Insular Cortex: $\Delta AI = 1.67$ with the formation of a control cluster at 1132 voxels, which may reflect an overbalancing of somatosensory integration; Anterior Cingulate Cortex: complete disappearance of ΔAI activation = 5.62, which indicates a decrease in affective discomfort.

Our data are supported, in part, by current research (e. g, Fan 2022 [1] and Vanneste et al. (2016)[22], indicating a decreased in neural hyperactivity and improved sensory integration. Further research should be aimed at clarifying the mechanisms of action and assessing the long-term effect of this method. This approach has the potential to be integrated into comprehensive tinnitus therapy, especially in patients who experience significant emotional or cognitive discomfort.

REFERENCES

1. Chen J, Fan L, Cai G et al. Altered amplitude of low-frequency fluctuations and degree centrality in patients with acute subjective tinnitus: a resting-state functional magnetic resonance imaging study. J Integr Neurosci. 2022;21(4):116. doi:10.31083/j.jin2104116. DOI
2. Boyen K, De Kleine E, Van Dijk P, Langers DRM. Tinnitus-related dissociation between cortical and subcortical neural activity in humans with mild to moderate sensorineural hearing loss. Hear Res. 2014;312:48–59. doi:10.1016/j.heares.2014.03.001. DOI
3. Elgoyhen AB, Langguth B, De Ridder D. Tinnitus: perspectives from human neuroimaging. Nat Rev Neurosci. 2015;16(10):632–642. doi:10.1038/nrn4003. DOI
4. Eggermont JJ. The auditory cortex and tinnitus – a review of animal and human studies. European J Neuroscie. 2015;41(5):665–676. doi:10.1111/ejn.12759. DOI
5. Ghodratitoostani I, Zana Y, Delbem ACB. Theoretical tinnitus framework: a neurofunctional model. Front Neurosci. 2016;10:370. doi:10.3389/fnins.2016.00370. DOI
6. Haider HF, Bojić T, Ribeiro SF, Paço J. Pathophysiology of subjective tinnitus: triggers and maintenance. Front Neurosci. 2018;12:866. doi:10.3389/fnins.2018.00866. DOI
7. Han Q, Zhang Y, Liu D et al. Disrupted local neural activity and functional connectivity in subjective tinnitus patients: evidence from resting-state fMRI study. Neuroradiology. 2018;60(3):291–299. doi:10.1007/s00234-018-2087-0. DOI
8. van der Wal A, Michiels S, Van de Heyning P et al. Treatment of Somatosensory Tinnitus: A Randomized Controlled Trial Studying the Effect of Orofacial Treatment as Part of a Multidisciplinary Program. J Clin Med. 2020;9(3):705. doi:10.3390/jcm9030705. DOI
9. van der Wal A, Michiels S, Van de Heyning P et al. Reduction of Somatic Tinnitus Severity is Mediated by Improvement of Temporomandibular Disorders. Otol Neurotol. 2022;43(3):e309–e315. doi:10.1097/MAO.0000000000003446. DOI
10. De La Torre Canales G, Christidis N, Grigoriadis A et al. Associations between temporomandibular disorders and tinnitus - a systematic review. Cranio. 2025;43(6):969-985. doi:10.1080/08869634.2024.2404270. DOI
11. Dipalma G, Inchingolo AD, Pezzolla C et al. The association between temporomandibular disorders and tinnitus: evidence and therapeutic perspectives from a systematic review. J Clin Med. 2025;14(3):881. doi:10.3390/jcm14030881. DOI
12. Saczuk K, Kal W, Kaczała A et al. The Coexistence of Tinnitus and Temporomandibular Disorder: A Narrative Review on the Importance of an Interdisciplinary Approach. J Clin Med. 2024;13(23):7346. doi: 10.3390/jcm13237346. DOI
13. Myrhaug H. Parafunktionen im Kauapparat als Ursache eines otodentalen Syndroms. [Parafunctions in the masticatory system as a cause of otodental syndrome]. Quintessenz. 1969;20:117–121. (German)
14. Bury M, Nijakowski K, Majewska A et al. The Co-Occurrence of Temporomandibular Disorders in Patients Diagnosed with Tinnitus: A Systematic Review with Meta-Analysis. J Clin Med. 2025;14(6):1836. doi: 10.3390/jcm14061836. DOI
15. Bökel A, Fobbe A, Lesinski-Schiedat A, Sturm C. Exploring the Effects of Manual Therapy on Somatosensory Tinnitus and Dizziness: A Randomized Controlled Trial. J Clin Med. 2025;14(13):4579. doi: 10.3390/jcm14134579. DOI
16. Michiels S, Naessens S, Van de Heyning P et al. The Effect of Physical Therapy Treatment in Patients with Subjective Tinnitus: A Systematic Review. Front Neurosci. 2016:10:545. doi: 10.3389/fnins.2016.00545. DOI
17. Turner JA, Deyo RA, Loeser JD et al. The importance of placebo effects in pain treatment and research. JAMA. 1994;271(20):1609–1614.
18. Peter N, Serventi J, Neff P et al. (2025). Tinnitus in patients with orofacial complaints. Head Face Med. 2025;21(1):31. doi: 10.1186/s13005-025-00505-w. DOI
19. Bumann A, Lotzmann U. Funktionsdiagnostik und Therapieprinzipien. [Functional diagnostics and therapy principles]. 8th ed. Stuttgart: Thieme. 2015, p.372. doi:10.1055/b-002-54091. (German) DOI
20. Hu J, Cui J, Xu JJ et al. The neural mechanisms of tinnitus: a perspective from functional magnetic resonance imaging. Front Neuroscie. 2021;15:621145. doi:10.3389/fnins.2021.621145. DOI
21. Chang Y, Lee H, Kim K. Neural networks of tinnitus: a systematic review and meta-analysis of functional neuroimaging studies. NeuroImage: Clinical. 2020;27:102302. doi:10.1016/j.nicl.2020.102302. DOI
22. Vanneste S, Plazier M, van der Loo E et al. The neural correlates of tinnitus-related distress. NeuroImage. 2010;52(2):470–480. doi:10.1016/j.neuroimage.2010.04.029. DOI
23. Schecklmann M, Landgrebe M, Langguth B. Phenotypic characteristics of hyperacusis in tinnitus. PLoS One. 2014;9(1):e86944. doi:10.1371/journal.pone.0086944. DOI
24. De Ridder D, Elgoyhen AB, Romo R, Langguth B. Phantom percepts: tinnitus and pain as persisting aversive memory networks. Proc Natl Acad Sci U S A. 2011;108(20):8075–8080. doi:10.1073/pnas.1018466108. DOI
25. Worsley KJ. Statistical analysis of activation images. Functional MRI: An Introduction to Methods. New York: Oxford University Press. 2001, p.251–270. http://ndl.ethernet.edu.et/bitstream/123456789/45780/1/315.pdf [Accessed 13 April 2025]
26. Çorbacıoğlu ŞK, Aksel G. Receiver operating characteristic curve analysis in diagnostic accuracy studies: a guide to interpreting the area under the curve value. Turk J Emerg Med. 2023;23(4):195–198. doi:10.4103/tjem.tjem_182_23. DOI

27. Peres ASC, Lemos TW, Barros AKD et al. Performance quantification of clustering algorithms for false positive removal in fMRI by ROC curves. Sci Flo Brazil. 2017;33(1):31–41. doi:10.1590/2446-4740.03215. DOI
28. Revilla-León M, Zeitler JM, Kois DE, Kois JC. Utilizing an additively manufactured Kois deprogrammer to record centric relation: A simplified workflow and delivery technique. J Prosthet Dent. 2024;132(1):20-25. doi: 10.1016/j.prosdent.2022.04.034. DOI

CONFLICT OF INTEREST

The Authors declare no conflict of interest

CORRESPONDING AUTHOR

Vasil Pekhno
Shupyk National Healthcare University of Ukraine
9 Dorohozhytska St, 04112 Kyiv, Ukraine
e-mail: Pekhnyo@ukr.net

ORCID AND CONTRIBUTIONSHIP

Vasil Pehnyo: 0000-0002-0075-6225 A B C D E F
Nataliia Savychuk: 0000-0001-9532-665X E F
Oleksandr Bida: 0000-0002-6038-6545 B
Stanislav Riebienkov: 0000-0001-8116-5277 B
Ivan Riabko: 0009-0000-6748-8686 C
Roman Sulik: 0000-0002-0487-3357 E

A – Work concept and design, B – Data collection and analysis, C – Responsibility for statistical analysis, D – Writing the article, E – Critical review, F – Final approval of the article

RECEIVED: 21.04.2025
ACCEPTED: 22.11.2025